Article

Effect of Hot Mixing Duration on Blending, Performance, and Environmental Impact of Central Plant Recycled Asphalt Mixture

Jie Gao [1], **Yuquan Yao** [2,*] , **Jinhua Huang** [3], **Jiangang Yang** [1], **Liang Song** [4,5], **Jing Xu** [1] and **Xinhu Lu** [6]

1 School of Civil Engineering and Architecture, East China Jiaotong University, Nanchang 330013, China;
   gaojie@ecjtu.edu.cn (J.G.); 2851@ecjtu.edu.cn (J.Y.); jingxv@ecjtu.edu.cn (J.X.)
2 School of Highway, Chang'an University, Xi'an 710064, China
3 School of Transportation Engineering, East China Jiaotong University, Nanchang 330013, China;
   2020138086100012@ecjtu.edu.cn
4 School of Transportation Engineering, Xinjiang University, Urumqi 830049, China; slpl@sohu.com
5 Xinjiang Communications Investment Group Construction Management Co., Ltd., Urumqi 830099, China
6 Xinjiang Transportation Investment (Group) Co., Ltd., Urumqi 830006, China; luxinhu@sina.cn
* Correspondence: 2020021063@chd.edu.cn

Abstract: When using a high concentration of reclaimed asphalt pavement (RAP) in a recycled hot-mix asphalt mixture (RHMA), the degree of blending of the reclaimed asphalt binder significantly affects the performance of the RHMA. Hence, it is essential to know the degree of blending of the RAP and its effect on the performance and the environmental impact of RHMA in order to determine the optimal mixing duration. To this end, the dispersion of reclaimed asphalt was observed using artificial RAP and the image analysis method, and the blending of reclaimed asphalt in RHMA with different mixing durations was also evaluated using physical properties tests, a rheometer test, a Fourier-transform infrared spectroscopy (FTIR) test, a gel permeation chromatography (GPC) test, and an atomic force microscope (AFM) test. The performance of RHMA with the different mixing durations in the plant and in the laboratory was tested using a Marshall stability test, rutting resistance test, freeze–thaw splitting test, and low-temperature bending beam test. In addition, the environmental impact of RHMA at different mixing durations was evaluated, and the optimal mixing duration was determined. The results showed that the mixing duration had a significant influence on the dispersion and blending of reclaimed asphalt in RHMA. The longer the mixing duration was, the higher the dispersion and the degree of blending of the reclaimed asphalt in the RHMA were. With the increase in the mixing duration, the properties, chemical composition, and micromorphology of the blended asphalt binder tended to become similar to those of reclaimed asphalt. The performance of RHMA was improved with the increase in mixing duration; however, the energy consumption and CO_2 emissions for the RHMA increase significantly with the increase in mixing time. The recommended optimal mixing durations in the mixing plant and in the laboratory were found to be 60 s and 90 s, respectively, considering the environmental impact, the RHMA production efficiency, and the performance of the RHMA.

Keywords: reclaimed asphalt pavement (RAP); recycled hot-mix asphalt mixture (RHMA); reclaimed asphalt; dispersion and blending; mixing duration

1. Introduction

In recent years, reclaimed asphalt pavement (RAP) has been widely used in pavement preservation, maintenance, and reconstruction due to the significant economic and environmental benefits [1–7]. In Europe, statistics from the European Asphalt Pavement Association (EAPA) show that 47% of RAP was used to produce recycled hot-mix asphalt mixture (RHMA) [8]. In the United States, the National Asphalt Pavement Association

(NAPA) reports that 84% of RAP was used in asphalt applications [8]. In general, RAP is widely used around the world and the percentage of RAP utilized in RHMA exceeds 30%, while in Europe, the United States, and Japan, it exceeds 80% [9]. Consequently, the performance of RHMA must be considered in order to ensure its economic and environmental advantages.

Hou et al. [10] concluded that RAP contains both aggregate and asphalt binder, and the properties of asphalt deteriorate due to long-term aging during road operation. In addition, the aged asphalt binder is very stiff compared to the fresh asphalt, and thus causes a change in the performance of RHMA. It has been reported that RHMA containing no more than 20% RAP has similar performances to conventional hot-mix asphalt (HMA). When the proportion of RAP incorporated is greater than 20%, the low-temperature crack resistance and anti-fatigue performance of RHMA deteriorate compared to HMA [11,12]. In order to produce RHMA with higher RAP content, it is essential to improve the uniformity of RAP dispersion and blending [10].

Currently, academics classify the blending of reclaimed asphalt in RHMA into three categories: full blending, partial blending, and black rock [13]. In this context, researchers have carried out series of studies considering the temperature, mixing process, RAP content, etc., and the blending degree of aged and virgin asphalt in RHMA has also been evaluated and calculated. Xu et al. [14] used the improved Hirsch dynamic modulus prediction model to quantitatively characterize the degree of blending of RHMA and studied the effects of mixing temperature and RAP contents on the degree of blending. The study revealed that the degree of blending between the aged and virgin asphalt binder could not reach 100% at the different mixing temperatures and RAP contents studied. In addition, the degree of blending influences the performance of RHMA. Ashtiani et al. [15] studied the degree of blending of RHMA containing different proportions of RAP and recycled asphalt shingles (RAS) using the Hirsch dynamic modulus prediction model and found that the aged asphalt binder from RAS and RAP blended with the virgin asphalt at rates of less than 40% and 60%. Kaseer et al. [16] found that aged asphalt coatings on RAP blended at 50% to 95% under 140 °C and 150 °C, with higher mixing temperatures leading to higher degrees of blending. Shirodkar et al. [17] studied the properties of blended asphalt binder and proposed a method to assess the degree of blending using asphalt rheology. They suggested that the degrees of blending of aged asphalt for 25% and 35% RAP by the weight of the aggregates reached 70% and 96%. Further, many scholars have tested chemical components and optical methods for determining RAP binder blend degrees, including FTIR, GPC, AFM, SEM, FM, and CT scans. [10]. Vassaux et al. [18] used the attenuated total reflection method to study the degree of blending of aged asphalt with various mixing temperatures and durations. The study reported that longer mixing durations improved the binder blending. Ding et al. [19] used FM to determine the blending degree of RAP and concluded that partial blending occurred in the RAP and RHMA, and the warm-mix technology showed a slightly higher blending degree compared to the hot mix. Bowers et al. [20] studied the influences of mixing duration and temperature using GPC. The blending degree was evaluated for a "fine" aggregate RAP and the test results showed that the maximum blending degree for RAP was below 80%. Solaimanian and Chen [21] used AFM to investigate the blending degree of RAP binder and virgin asphalt based on the surface morphology and the Derjaguine–Muller–Toporov (DMT) modulus. Rinaldini et al. [22] investigated the blending of recovered asphalt with fresh asphalt using CT and SEM and found that the blending degree of RAP was not homogeneous throughout the sample. Xu et al. [23] used the staged extraction method and the AFM imaging technique to study the blending of RAP and virgin asphalt with different mixing temperatures and residence times. The study found that the mixing temperature and residence time have significant effects on the blending degree and the non-homogenous blending between RAP and virgin binders. In general, the abovementioned studies show that the type of blending that RAP undergoes in RHMA is partial blending.

Previous studies have evaluated the blending degree of RAP in RHMA by considering the mixing temperature, mixing duration, RAP content, and blending method. RHMA and blended asphalt perform differently depending on the degree of blending of RAP. However, only a handful of studies have considered the effects of RAP aggregate gradation and RHMA gradation when used in practice. In addition, there are few studies that have been conducted on both properties: the chemical components of blended asphalt and the performance of RHMA considering the blending degree of RAP. There are also few studies that have been conducted to determine the optimal mixing duration of RHMA in the plant and in the laboratory that consider the performance and the environmental impact of RHMA. Hence, the objectives of the study were to observe and evaluate the dispersion and blending of reclaimed asphalt and to analyze its effect on the properties, chemical composition, and morphology of blended asphalt, as well as the performance of RHMA. In practice, the blending method, mixing temperature, and RAP content are constant, while the mixing duration of RHMA can be adjusted. Therefore, this study considered the effects of different mixing durations on the dispersion and blending of reclaimed asphalt with the optimal temperature and mixing method. Furthermore, the optimal mixing duration of RHMA in the plant and the laboratory, considering the performance and the environmental impact, was determined. The framework of this study is summarized and illustrated in Figure 1.
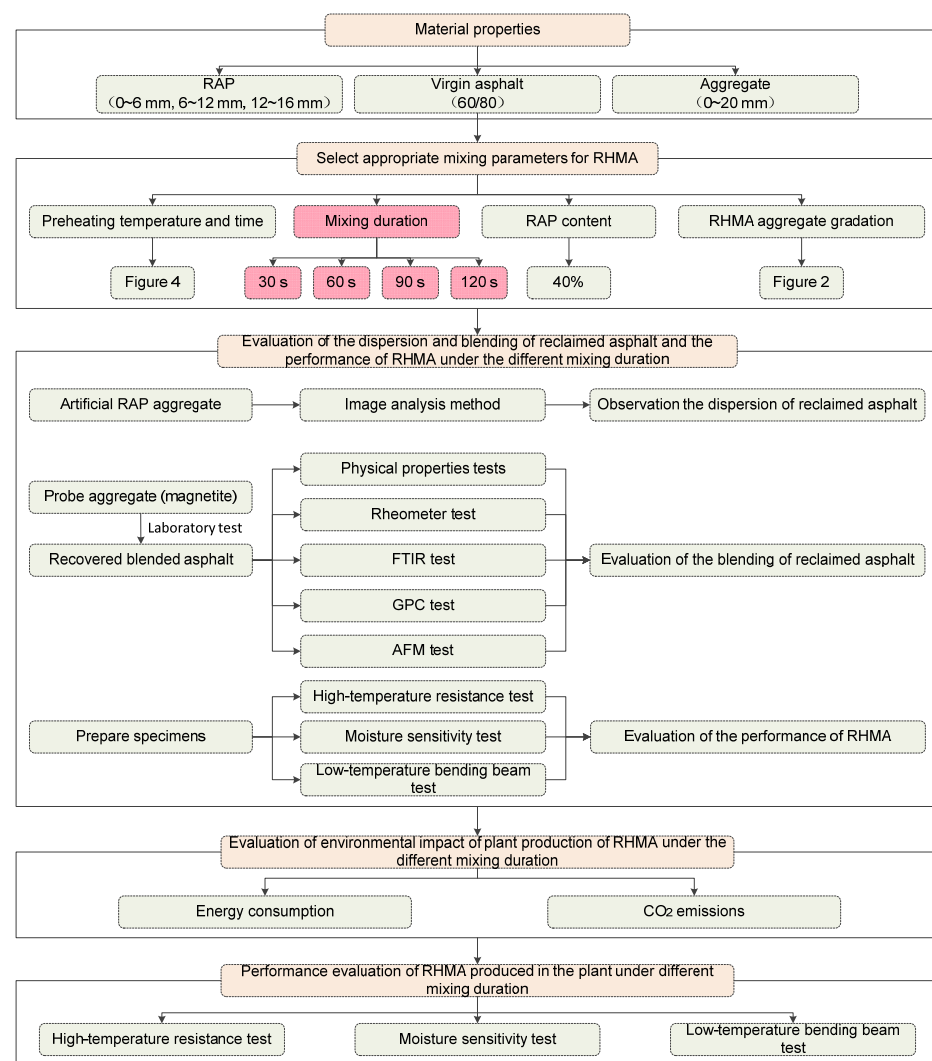

Figure 1. The framework of this study.

2. Materials and Methods

2.1. Materials

The materials used in this study included #70 matrix asphalt (virgin asphalt), virgin aggregate, and RAP. The performance indexes of #70 virgin asphalt according to the Chinese specification entitled Standard Test Methods of Bitumen and Bituminous Mixtures for Highway Engineering (JTG E20-2011) [24] are shown in Table 1. The virgin aggregate was limestone with a particle size of 0~20 mm, which was sieved according to the sieve size before being used in the preparation of recycled asphalt mixes. The performance indexes of virgin aggregate were tested following the Testing Methods of Aggregate for Highway Engineering (JTG E42-2005) [25], and Table 2 shows the results. In addition, RAP was obtained from the AC-20 middle surface layer of the Sanming section of the Fuzhou–Yinchuan Expressway in Fujian Province, China, and divided into three types (0~6 mm, 6~12 mm, 12~16 mm) through crushing and screening. The gradation, asphalt content, and performance indexes of RAP were obtained by following the Technical Specifications for Highway Asphalt Pavement Recycling (JTG T 5521-2019) [26] and are listed in Tables 3 and 4. The performance indexes of all materials met the Technical Specifications for Construction of Highway Asphalt Pavements (JTG F40-2004) [27].

Table 1. Performance indexes of #70 virgin asphalt.

	Test Items	Test Results	Test Method
	Penetration, 25 °C, 0.1 mm	74.9	T0604
	Softening point, °C	50.1	T0606
	Ductility, 15 °C, cm	>100	T0605
	Viscosity, 60 °C, Pa·s	225	T0620
RTFOT	Penetration ratio, %	71.2	T0604
	Residual ductility, 10 °C, cm	32.5	T0605
	Mass loss, %	−0.03	T0610

Table 2. Performance indexes of virgin aggregate.

Aggregate Type	Test Items	Test Results	Test Method
Coarse aggregate	Specific gravity	2.751	T0304
	Flakiness and elongation particles, %	11.4	T0312
	Crushing value, %	12.6	T0316
	Los Angeles abrasion, %	13.7	T0317
	Water absorption, %	0.5	T0304
Fine aggregate	Specific gravity	2.715	T0328
	Sand equivalent, %	70.1	T0334
Filler	Specific gravity	2.648	T0352

Table 3. Gradation and asphalt content of RAP before and after extraction.

Sieve Size/mm	12~16 mm		6~12 mm		0~6 mm	
	Before	**After**	**Before**	**After**	**Before**	**After**
16	100.0	100.0	100.0	100.0	97.9	100.0
13.2	100.0	100.0	100.0	100.0	60.1	78.5
9.5	100.0	99.9	85.2	92.2	4.9	32.6
4.75	74.5	96.8	6.6	26.0	0.4	18.4
2.36	35.6	62.9	1.9	17.4	0.1	13.3
1.18	19.6	45.8	1.0	14.9	0.1	10.9
0.6	9.3	36.4	0.5	12.3	0.1	9.5
0.3	2.8	26.1	0.2	9.6	0.1	7.4
0.15	1.2	19.2	0.2	7.5	0.1	5.7
0.075	0.3	14.9	0.0	6.0	0.0	4.5
Asphalt content, %	-	2.32	-	3.16	-	7.86

Table 4. Performance indexes of RAP.

Material Type	Indicators	Test Results	Test Method
RAP	Moisture content, %	0.57	T0307 and T0334
	Sand equivalent, %	86.7	
Asphalt in RAP	Penetration, 25 °C, 0.1 mm	28.5	T0604
	Softening point, °C	71.2	T0606
	Ductility, 15 °C, cm	23.1	T0605
	Viscosity, 60 °C, Pa·s	1980	T0620
Coarse aggregate	Crushing value, %	14.7	T0316
	Flakiness and elongation particles, %	13.8	T0312
Fine Aggregate	Angularity	32.1	T0345

2.2. Sample Preparation

Mixing durations of 30 s, 60 s, 90 s, and 120 s were studied to observe and evaluate the dispersion and blending of reclaimed asphalt under the different mixing conditions. First, the effect of mixing duration on the dispersion of aged asphalt on RAP surfaces was investigated; then, the blending of aged asphalt and virgin asphalt with different mixing durations was evaluated; lastly, the performance of the RHMA was evaluated.

During mixing, the aged asphalt on RAP surfaces adheres to the virgin aggregate and disperses. In addition, Yang et al. [5] found that the agglomerated particles present in RAP affect the dispersion of aged asphalt. Therefore, to better observe the dispersion of aged asphalt containing agglomerated RAP during the mixing process, an artificial RAP aggregate was produced using 12~16 mm RAP and 0~6 mm RAP asphalt mastic. The particle size of the virgin aggregate used in the test was 9.5~26.5 mm, and the amount of virgin aggregate was determined according to the proportion in the design gradation of RHMA, as shown in Figure 2. To observe the dispersion of reclaimed asphalt with different mixing durations, an asphalt mixture containing artificial RAP was produced at a mixing temperature of 175 °C over 30 s, 60 s, 90 s, and 120 s after the virgin aggregate had been heated by the oven at 190 °C for at least 2 h; the virgin asphalt was not added to the asphalt mixture during mixing. Finally, the distribution of aged asphalt on the surface of the virgin aggregate was photographed and observed for the different mixing durations, and the test process is shown in Figure 3.
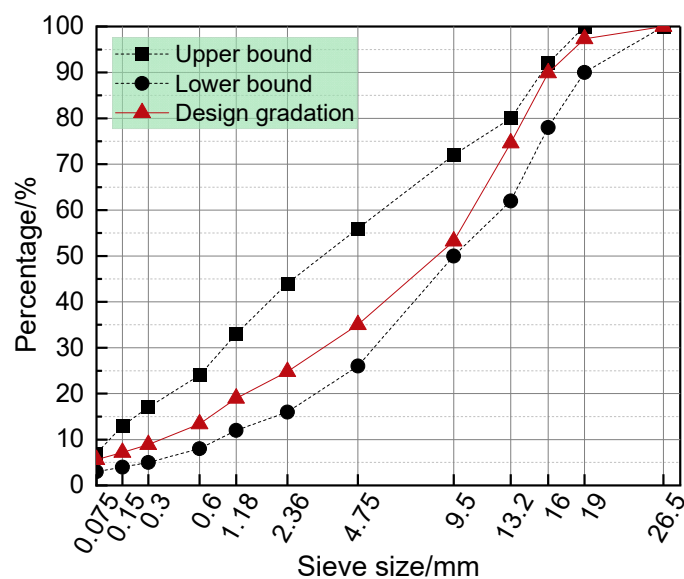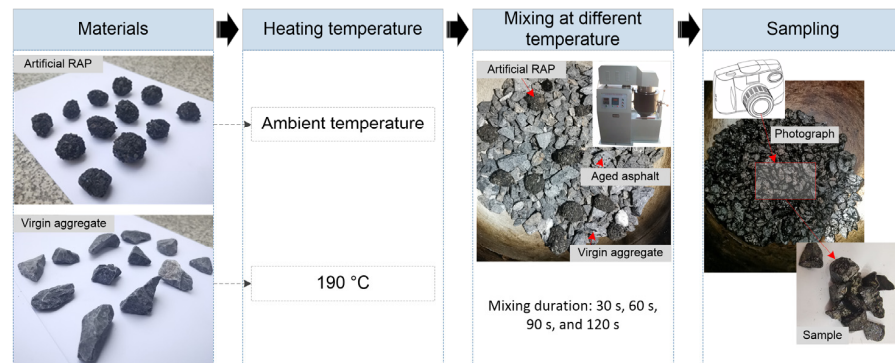

Figure 2. Grading curve of RHMA.

Figure 3. Test process for aged asphalt distribution with different mixing durations.

Magnetite was used as a probe aggregate to determine the blend of reclaimed asphalt with the different mixing durations and assess the blending of asphalt, and the blended asphalt was extracted from magnetite aggregate using trichloroethylene as a solvent with the centrifuge method and recovered from the solution with a rotary evaporator. In addition, the particle size of the magnetite used in this study was 16~26.5 mm, and it was used to replace a certain amount of the virgin aggregate in the RHMA. To investigate the blending of reclaimed asphalt and virgin asphalt with different mixing durations, RHMA containing 40% RAP and 60% virgin aggregate was designed, and the asphalt content of the RHMA was 4.4%. In accordance with the design grading (Figure 2), the mixing process for RHMA was designed as follows: (1) RAP was dried in the oven at 130 °C for no more than 2 h, and the virgin aggregate (including magnetite) and virgin asphalt were heated in the oven at 190 °C and 150 °C for at least 2 h; (2) the RAP, virgin aggregate, magnetite, and virgin asphalt were added to the mixer at 175 °C, and different mixing durations were used; (3) lastly, the filler was added to the mix at 175 °C for 30 s, and the RHMA was produced. Figure 4 illustrates the workflow which involved testing, sampling, and then testing again. Based on the above experiment, the blended asphalt containing reclaimed asphalt and virgin asphalt was recovered, and its performance and chemical composition could be tested.

Figure 4. The process of blending asphalt with different mixing durations.

To evaluate the effects of the various mixing durations on the performance of RHMA when blended with reclaimed asphalt, a Marshall stability test, rutting resistance test, moisture sensitivity test, and the bending test was conducted based on the aforementioned material composition of RHMA.

2.3. Methods

2.3.1. Image Analysis Method

The dispersion images of aged asphalt covered in RAP were obtained with different mixing durations, as shown in Figure 3. From the image, it can be seen that the aged asphalt covered the virgin aggregate surface, and the difference was significant. To evaluate the dispersion of aged asphalt with different mixing durations, five images were obtained, and the regions covered with aged asphalt on the surface of the virgin aggregate were distinguished using Image Pro Plus software. This process was performed by converting the original digital images to grayscale images, and the aged asphalt could be identified by using a grayscale threshold of 0 to 52. In addition, the areas of virgin aggregate and those where aged asphalt covered the virgin aggregate were used to evaluate the degree of dispersion with the different mixing durations, which was calculated as shown in Equation (1):

$$A_R = \frac{A_{\text{aged asphalt}}}{A_{\text{virgin aggregate}}} \times 100 \tag{1}$$

where A_R refers to the area ratio of the distribution of the aged asphalt in the virgin aggregate (%); $A_{\text{aged asphalt}}$ refers to the area of the aged asphalt covered in the virgin aggregate (cm^2); and $A_{\text{virgin aggregate}}$ refers to the total area of the virgin aggregate (cm^2).

2.3.2. Asphalt Binder

Investigation into the performance of asphalt binder recovered from RHMA with different mixing durations was conducted based on physical properties tests and rheometer tests. In addition, the microscopic composition of the asphalt binder was tested using a Fourier-transform infrared spectroscopy test, gel permeation chromatography test, and atomic force microscopy test.

Physical Properties Tests

The penetration, softening point, and ductility were used to evaluate the physical properties of the recovered asphalt, and these tests were conducted using an automated test device according to the JTG E20-2011 standard [24].

Rheometer Test

A DHR-1 dynamic shear rheometer was used to determine the rheological properties of the blended asphalt. Angular frequencies between 0.1 and 100 rad/s were tested at 15, 25, and 35 °C. In addition, the asphalt samples were tested using a parallel plate with a diameter of 8 mm and gap of 2 mm. Based on the fact that the complex modulus of the asphalt binder decreased to 95% of its initial value before the frequency sweep tests, strain sweep tests were conducted to determine its linear viscoelastic region. After obtaining the limited strain, the frequency sweeps tests were carried out. In addition, the rheological master curve was established at 25 °C (the representative temperature of asphalt pavement in the service cycle is 25 °C [28]) based on the test results. A sigmoidal model was used to construct the modulus master curve, and a double-logistic mathematical function was used to model the phase angle master curve [29].

The low-temperature rheological properties of the blending asphalt were examined by using a TE-BBR bending beam rheometer from Canon Company, and the bending creep stiffness S and creep rate m of the blending asphalt were calculated by using a bending creep test. Four parallel tests were conducted for each group at −12 °C and −18 °C

with the length, width, and height of asphalt specimens being 127 mm, 12.7 mm, and 6.35 mm, respectively.

FTIR Test

The reaction of the reclaimed asphalt with virgin asphalt was accompanied by a change in the concentrations of the functional groups, including carboxylic acids, sulfoxides, ketones, and anhydrides [30]. Molecular functional groups are atomic groups within molecules that possess unique properties, regardless of the presence of other atoms [31]. In this test, the chemical functional groups of blended asphalt shared between reclaimed and virgin asphalt were identified based on the absorption intensities using an FTIR test, and the degree of blending was evaluated. To conduct the test, the four blending asphalt samples recovered from magnetite were placed on the crystal using a metal spatula. The spectra test range was 4000–600 cm^{-1}, and a resolution of 4 cm^{-1} was used with 24 scans. Previous studies [32,33] show that the C=O bond (carbonyl region) and S=O bond (sulfoxide) e change with the aging of the asphalt, and aged asphalt has higher C=O and S=O peaks while virgin asphalt has a lower peak. Hence, in this study, the C=O and S=O functional groups were used to indicate the degree of blending of reclaimed and virgin asphalt with different mixing durations. To quantify the C=O and S=O functional groups based on the FTIR curve, the carbonyl index (CI) and sulfoxide index (SI) were proposed and calculated using Equations (2) and (3). In addition, it should be noted that all spectra were normalized to the band with the highest intensity in the bitumen spectrum; i.e., the aliphatic band at 2920 cm^{-1}. Min-max normalization in the range from 3007.946 to 2766.898 cm^{-1} was carried out, which reduced the impact of any errors coming from the FTIR crystal [34]. Equations (2) and (3) are as follows:

$$CI = \frac{A_{C=O}}{A_{\text{Reference}}} \times 100 \tag{2}$$

$$SI = \frac{A_{S=O}}{A_{\text{Reference}}} \times 100 \tag{3}$$

where CI represents the carbonyl index (%); SI represents the index of the sulfoxide group (%); $A_{C=O}$ represents the area of the C=O functional group at the wavelengths from 1722.357 to 1672.210 (cm^{-1}); $A_{S=O}$ represents the area of the S=O functional group at the wavelengths from 987.112 to 1057.611 (cm^{-1}); and $A_{\text{Reference}}$ represents the area of a reference position at wavelength from 3007.946 to 2766.898 (cm^{-1}) [31,35].

GPC Test

The GPC test was used to determine the molecular weight distribution for the asphalt binder. Previous studies have shown that the molecular weight of asphalt binder can be separated into three major fractions: large molecule size (LMS), medium molecule size (MMS), and small molecule size (SMS) [20]. Therefore, the change in the blending asphalt can be characterized by the molecular weight due to the difference in the molecular weight between reclaimed and virgin asphalt. A Waters 1515 gel permeation chromatograph was used to conduct the test and the chromatogram was obtained. According to the chromatogram, which was divided into 13 slices, the first 5 segments had LMS, segments 6–9 had MMS, and segments 10–13 had SMS. In addition, the LMS percentage was used to quantitatively evaluate the influence of the blending asphalt binder with different mixing durations, and the calculation is shown in Equation (4):

$$I_{LMS} = \frac{A_{LMS}}{A_C} \times 100 \tag{4}$$

where I_{LMS} represents the macromolecular content index (%); A_{LMS} indicates the basis of the area beneath the chromatogram curve; and A_C represents the total area of the chromatogram regions containing different molecule sizes.

AFM Test

The AFM imaging technique was used in this study to capture the topography of the different blended asphalts and to analyze the degree of blending of the reclaimed and virgin asphalt with the different mixing durations. In this test, the surface topography was observed using a Bruker Icon atomic force microscope. The peak force, feedback gain, and probe scan rate were 30 nN, 20, and 1 Hz, respectively. To prepare samples, various asphalt binders were first heated, and a small amount of asphalt binder was put on a slide; next, the slide was heated in an oven at 110 °C for 2 min, and then stored at 25 °C ambient temperature and 25% relative humidity for another 24 h [36]. Finally, three parallel tests were carried out for each group and the microscopic image was recorded with a 20 μm × 20 μm scan size and a pixel resolution of 512 ppi × 512 ppi.

In previous studies, bee-like structures have been observed in asphalt AFM images, which were influenced by the composition of the saturate, aromatic, resin, and asphaltene (SARA) components) [37]. Therefore, to quantitatively represent the effect of asphalt blending using AFM images, the density and average area index of the bee-like structures were calculated with NanoScope Analysis software and computer-imaging analysis software and analyzed in two-dimensional images. Following our previous study [38], the image processing and the calculation process are shown in Figure 5.
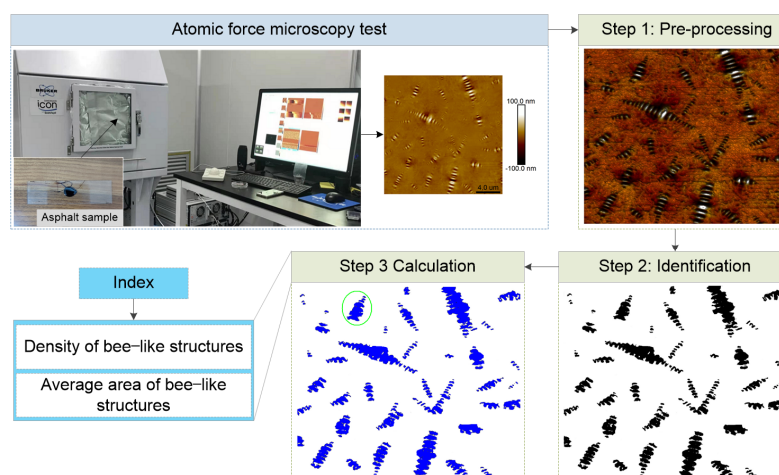

Figure 5. The analysis process for the asphalt micro-morphologic image.

2.3.3. Asphalt Mixture

High-Temperature Resistance Test

The Marshall stability test and the rutting test were carried out to determine the performance of the RHMA under high temperatures.

The Marshall stability test was performed using Marshall stability equipment according to the specification of the JTG E20-2011 standard [24], and the Marshall stability and flow value of the specimen were tested. The Marshall stability was tested under a loading rate of 50 mm/min at 60 °C after the specimens of 100 mm diameter and 63.5 mm height were immersed in a water bath at a temperature of 60 °C for 30~40 min. In addition, the Marshall stability was regarded as the maximum load of the specimen that would cause the failure of the specimen, and the flow value was determined as the vertical deformation of the specimen under the point of failure.

A rutting resistance test was conducted to determine the dynamic stability of the RHMA. In addition, three rutting samples (300 mm × 300 mm × 50 mm) of the mixtures were produced for the RHMA with different mixing durations. The rutting test was carried out according to the JTG E20-2011 standard [24], and the deformation of the

specimen was recorded during the test. The dynamic stability index was calculated using the following equation:

$$DS = \frac{(t_2 - t_1) \times N}{d_2 - d_1} \tag{5}$$

where DS refers to the dynamic stability of mixes (cycles/mm); the value of t_1 was 45 min; that of t_2 was 60 min; N is the rotation speed of the wheel (42 rpm/min); d_1 is the rutting depth at t_1 (mm); and d_2 is the rutting depth at t_2 (mm).

Moisture Sensitivity Test

A freeze–thaw splitting test was conducted to determine the moisture sensitivity of the RHMA. Six specimens were prepared and equally divided into unconditioned and conditioned groups, and the test was conducted according to the JIG E20-2011 standard [24]. The tensile strengths of the specimens before and after conditioning were calculated according to Equations (6) and (7):

$$TS = \frac{0.006287 \times P_T}{h} \tag{6}$$

where TS represents the tensile strength (MPa); P_T represents the maximal loading pressure (N); and h represents the height of the specimen (mm).

$$TSR = \frac{TS_{after}}{TS_{before}} \times 100 \tag{7}$$

where TSR represents the freeze–thaw splitting tensile strength ratio (%); TS_{after} represents the average tensile strength of the specimen after being vacuumed at 0.9 MPa for 15 min and transferred into a bath for 24 h at 60 °C, after which the tensile strength was tested after 2 h in the water bath at 25 °C (MPa); and TS_{before} represents the average tensile strength after the specimen was placed into the water bath for 2 h at 25 °C (MPa).

Low-Temperature Bending Beam Test

The low-temperature crack resistance of the RHMA was evaluated using a low-temperature bending beam test according to the JTG E20-2011 standard [24]. Six bending beam specimens with sizes of 250 mm × 30 mm × 35 mm were prepared and the test was conducted using a UTM-100 at −10 °C. The flexural tensile failure was calculated using Equation (8):

$$\varepsilon_B = \frac{6 \times h \times d}{L^2} \tag{8}$$

where ε_B refers to the maximum flexural strain after specimen failure ($\mu\varepsilon$); h refers to the height of the transverse section at the mid-span of the testing beam (mm); d refers to the deflection at the mid-span of the specimen during failure (mm); and L refers to the span of the specimen (mm).

3. Results and Analysis

3.1. Reclaimed Asphalt Dispersion with Different Mixing Durations

Figure 6 shows the dispersion of the aged asphalt on the virgin aggregate surface with different mixing durations. It is obvious that the variation in the area of the aged asphalt coating on the surface of the virgin aggregate increased with the increase in the mixing duration. In addition, the values of A_R were calculated as 22.9%, 37.6%, 53.7%, 66.5%, and 86.1% respectively, and the standard deviations were 2.1%, 5.7%, 5.6%, 6.2%, and 9.2%, respectively. Therefore, the mixing duration significantly affected the dispersion of the aged asphalt in the RAP over the virgin aggregate, and the longer mixing durations allowed the aged asphalt to spread sufficiently during the mixing process.
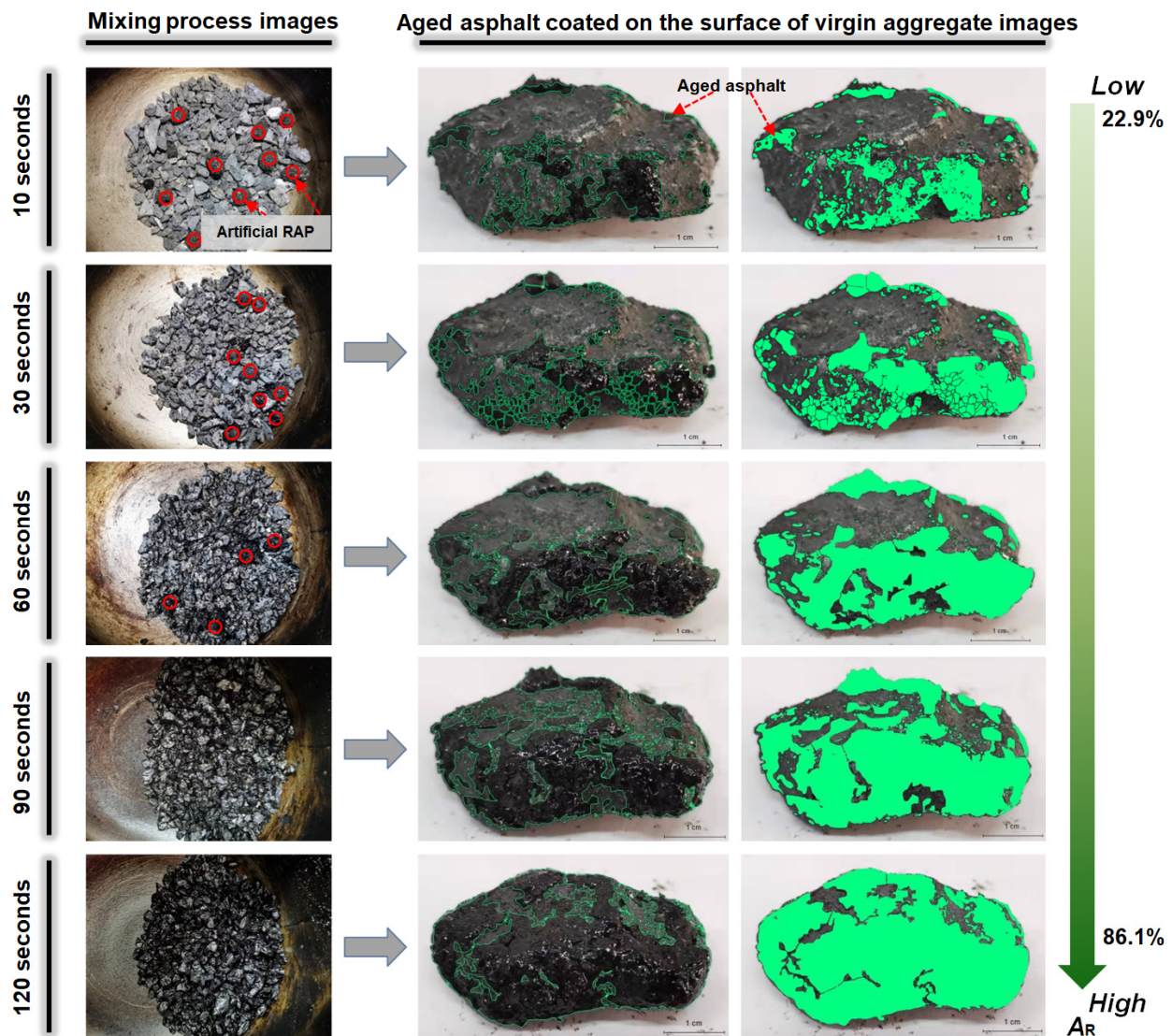
Figure 6. Dispersion of aged asphalt over the virgin aggregate surface with different mixing durations.

3.2. Performance and Chemical Composition of Blended Asphalt with Different Mixing Durations

3.2.1. Physical Properties Tests

Figure 7 presents the test results for the physical properties of the asphalt binder with different mixing durations. It is evident that the virgin asphalt significantly improved the physical properties of the aged asphalt. In addition, the penetration and ductility of the blended asphalt decreased with the increase in mixing duration compared to the virgin asphalt, while the softening point showed the opposite trend. According to the aforementioned results, the mixing duration affected the degree of dispersion of the aged asphalt during mixing, resulting in the physical properties of the blended asphalt becoming close to those of aged asphalt. Furthermore, the physical properties of the blended asphalt exhibited a lower range of changes with the increase in the mixing duration, indicating that the properties of the blended asphalt were becoming stable.
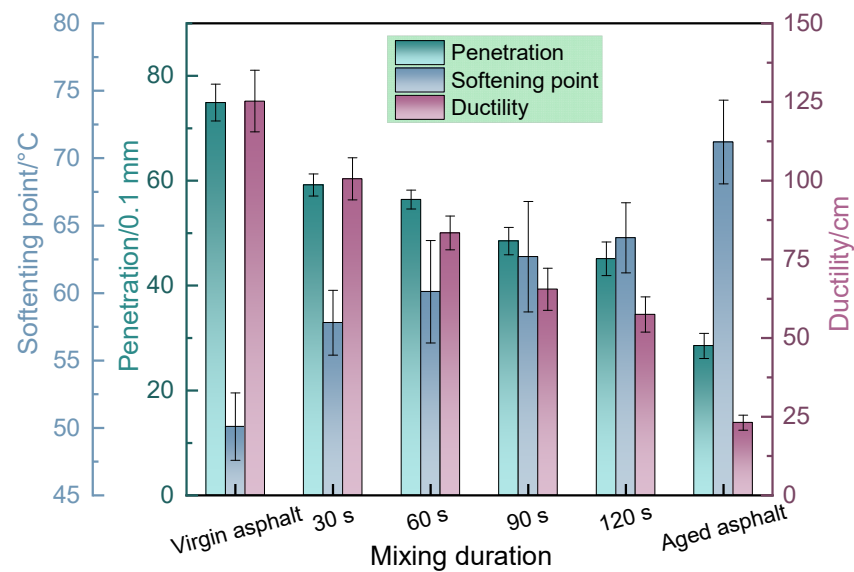
Figure 7. Test results for physical properties of asphalt binder.

3.2.2. Rheometer Test

The test results for the complex shear modulus and phase angle at the reference temperature of 25 °C for virgin asphalt, aged asphalt, and blended asphalt with different mixing durations are shown in Figure 8.
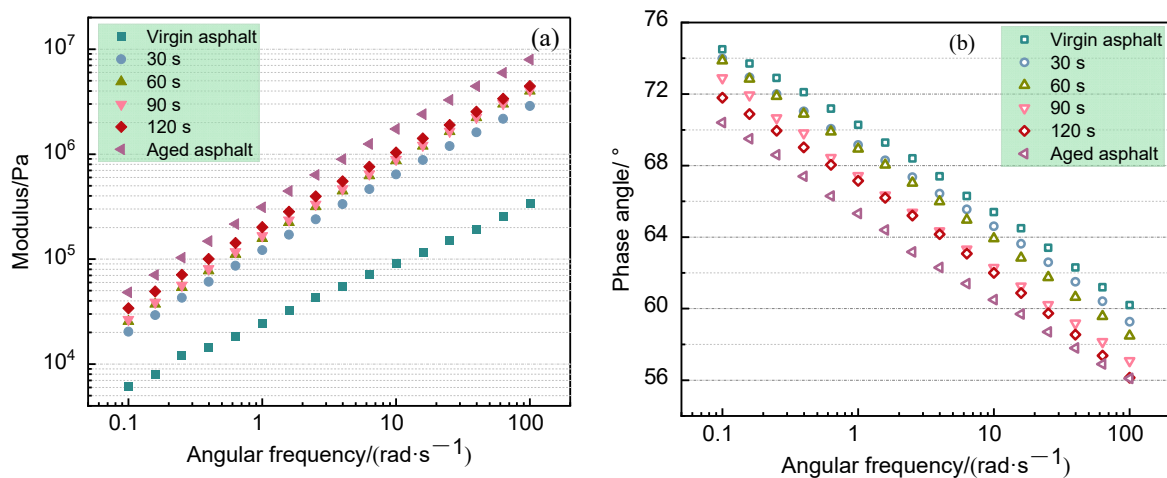

Figure 8. Rheological properties: (**a**) complex modulus master curves at 25 °C for blended asphalt with different mixing durations; (**b**) phase angle master curves at 25 °C for blended asphalt with different mixing durations.

As can be seen from Figure 8a, the maximum and minimum complex moduli were represented by aged asphalt and virgin asphalt, respectively, and the complex modulus of the blended asphalt increased with the increase in the mixing duration compared to virgin asphalt, indicating that the blended asphalt was gradually aging, and the blended asphalt was more resistant to rutting and had better high-temperature stability. It can also be seen from Figure 8a that, on a log scale, the increase in the complex modulus of the blended asphalt was more significant at a mixing duration of 30 s compared to the virgin asphalt, and the rate of increase decreased with the increase in the mixing duration. Figure 8b shows that the phase angle of the blended asphalt decreased with the greater mixing duration compared to virgin asphalt. In addition, the reductions in the phase angle decreased with longer mixing durations, which was consistent with the variation law of the modulus.

As the mixing duration increased, the stiffness modulus of the blended asphalt increased compared to the virgin asphalt (Figure 9). This indicates that the mixing duration resulted in the hardening of the blended asphalt and the low-temperature bending behavior weakened. In terms of the different mixing durations at different test temperatures, the growth range of the stiffness modulus decreased with increasing mixing durations. As the test temperature increased, the stiffness modulus S of the blended asphalt binder decreased, and the lower the temperature, the weaker the creep resistance of the asphalt was. The SHRP specify that the asphalt binder stiffness modulus should be lower than 300 MPa to ensure the low-temperature performance of an asphalt mixture. The mixtures of asphalt studied here had excellent properties at −12 °C and −18 °C, except for the asphalt binder recovered after 120 s of mixing.
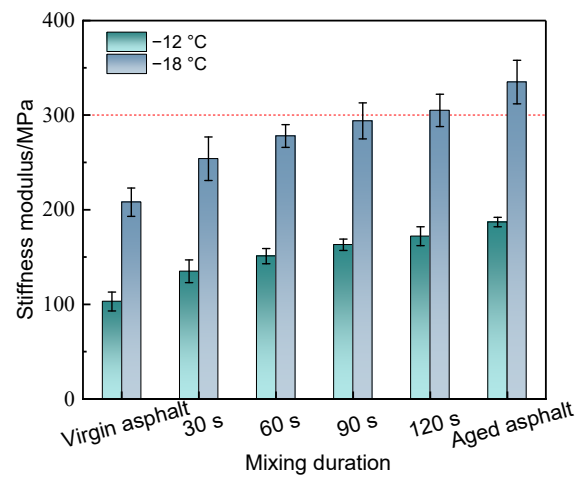

Figure 9. Variation in asphalt stiffness modulus S with different mixing durations at different temperatures.

According to Figure 10, the asphalt binder was more prone to breaking under stress at lower temperatures. The results of the tests showed that the blended asphalt's creep rate m decreased as the mixing duration increased and the asphalt's degree of aging increased, resulting in the low-temperature crack resistance decreasing. However, when the mixing duration was increased, the range of decline of the creep rate m decreased. In addition, the SHRP suggest that the creep rate m should be higher than 0.3. Thus, the asphalt binder including virgin asphalt, aged asphalt, and blended asphalt met the requirements at −12 °C; however, the blended asphalt with various mixing durations did not meet the specifications at −18 °C.
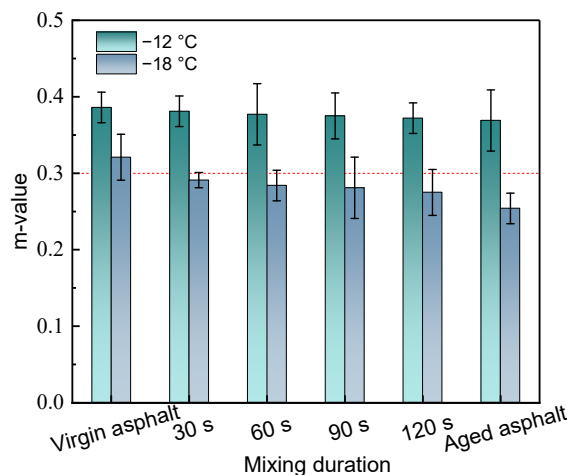

Figure 10. Variation in asphalt creep rate m with different mixing durations at different temperatures.

3.2.3. FTIR Test

Figure 11 demonstrates the test results for the infrared spectra of the different asphalts obtained with FTIR. The vibration peaks at 748 cm^{-1}, 811 cm^{-1}, 873 cm^{-1}, 1027 cm^{-1}, 1375 cm^{-1}, 1454 cm^{-1}, 1602 cm^{-1}, 1697 cm^{-1}, 2354 cm^{-1}, 2856 cm^{-1}, and 2920 cm^{-1} are apparent. In addition, the number of vibrational peaks shows that no new functional groups were produced during the fusion of the old and new asphalt. Based on the trend in the vibrational peaks, it is clear that there was a significant difference between the C=O (absorption peak at the wavelength of 1697 cm^{-1}) and S=O (absorption peak at the wavelength of 1027 cm^{-1}) curves of the different asphalts, and the intensity of the absorption peaks increased with the increase in the mixing duration. The absorption peak of the aged asphalt was the highest, followed by those of the blended asphalt and virgin asphalt.
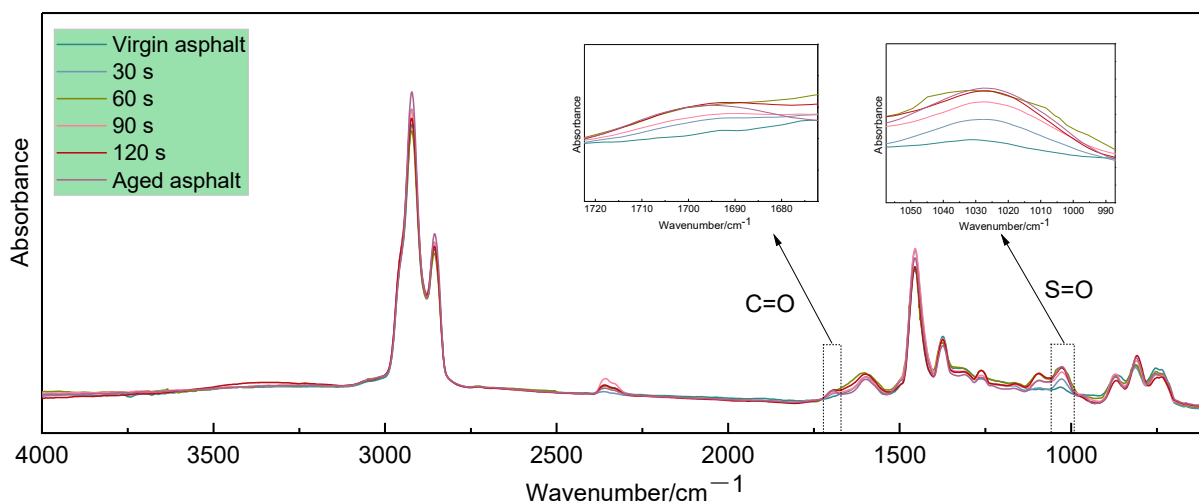

Figure 11. Infrared spectra of the asphalt binder with different mixing durations.

To evaluate the degree of blending of the asphalt binder containing aged and virgin asphalt in the FTIR test, the bond index (*CI* and *SI*) was calculated using Equations (2) and (3). Figure 12 shows that the carbonyl index *CI* and sulfoxide index *SI* were significantly increased after mixing at different times, with an increase of 116.4% and 218.3%, respectively, compared to the virgin asphalt. The carbonyl index *CI* and sulfoxide index *SI* in the virgin asphalt were the smallest, while the aged asphalt had the highest indexes. In addition, the range of increase of the carbonyl index *CI* and sulfoxide index *SI* in the blended asphalt decreased with the increase in the mixing duration.
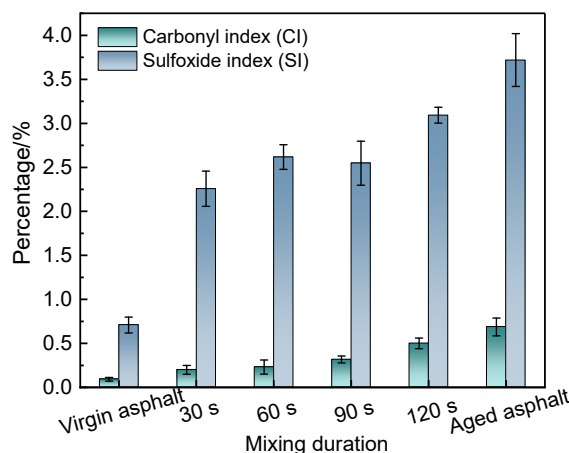

Figure 12. Variation in carbonyl index and sulfoxide index for the different asphalts.

3.2.4. GPC Test

Figure 13 shows the relative molecular mass distributions for aged asphalt, blended asphalt, and virgin asphalt, with the horizontal axis representing the logarithm of the average heavy molecular weight (M_w) and the vertical axis representing the asphalt content (M). The higher the degree of aging of the asphalt was, the larger the area of the curve distribution for the larger scale of molecular weight was, as shown in Figure 13. As Figure 14 shows, the LMS content in the asphalt binder was calculated to quantitatively evaluate the change in the asphalt molecular weight during mixing. According to Figure 14, aged asphalt had the highest LMS content while virgin asphalt had the lowest. When the mixing duration increased, the LMS content in the blended asphalt increased, suggesting that the aging asphalt was more prevalent in the blended asphalt.
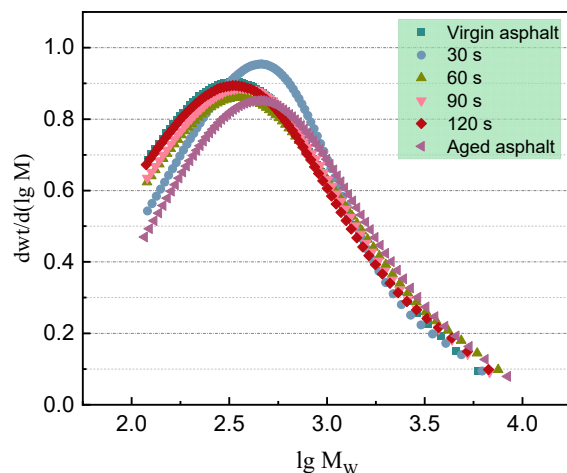
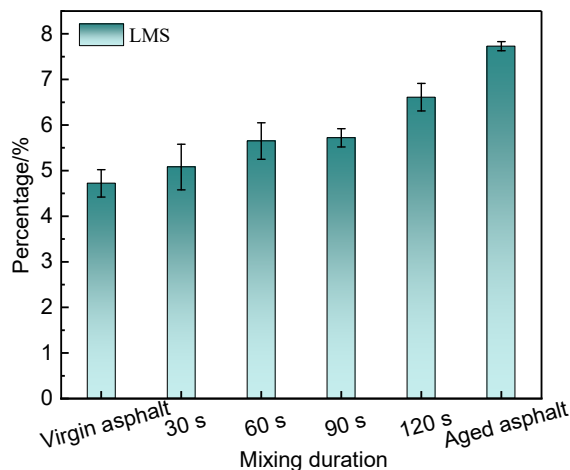**Figure 13.** Chromatograms of the asphalt binder with different mixing durations.

Figure 14. LMS content in the asphalt binder with different mixing durations.

3.2.5. AFM Test

AFM images of the virgin asphalt binder, aged asphalt binder, and blended asphalt binder recovered from magnetite aggregate are displayed in Figure 15. As can be seen from Figure 15a–f, the surface morphology of the different asphalt binders mainly had a bee-like structure, and the areas and numbers were different with different mixing duration. The number of bee-like structures decreased with the increase in the mixing duration, which shows that the components of the blended asphalt changed during the mixing process due to the bee-like structure being affected by the asphalt components (saturated fraction, aromatic fraction, resin, and asphaltene) [39,40]. In addition, the number of

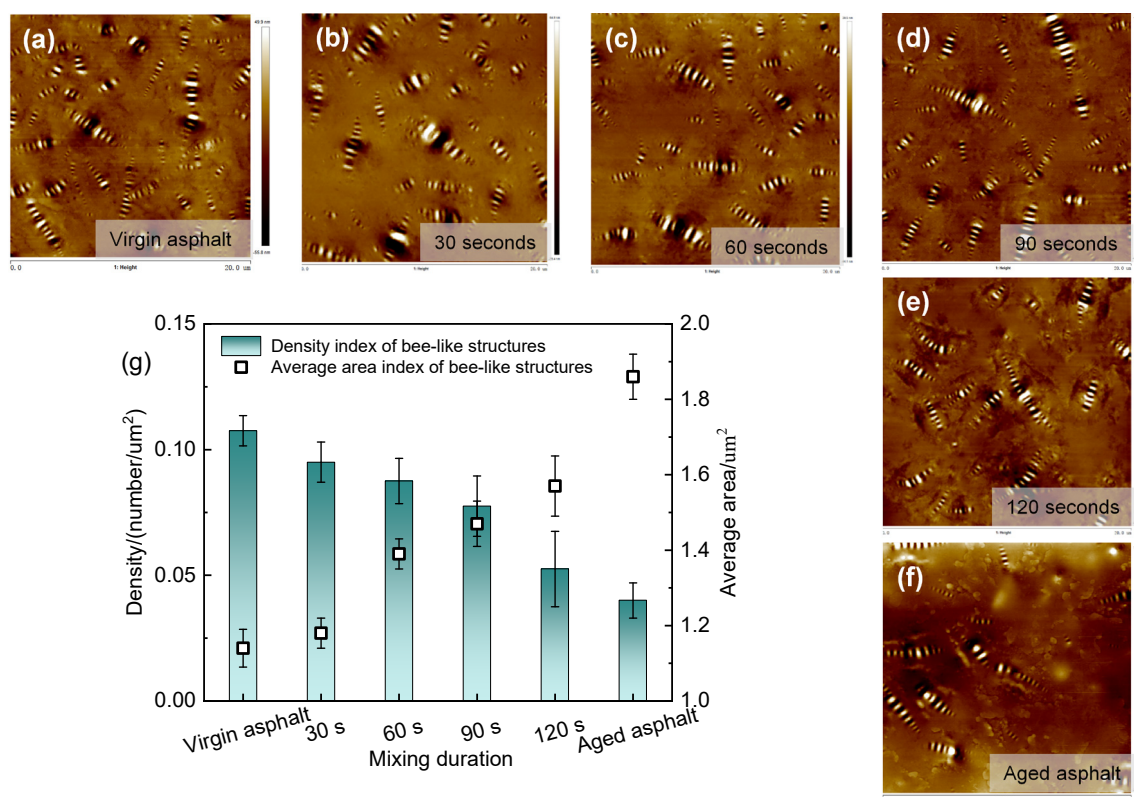bee-like structures in the virgin asphalt was the highest, while that of aging asphalt was the lowest.

Figure 15. AFM image test and analysis results: (**a**) virgin asphalt binder; (**b**) blended asphalt binder under the 30 s mixing duration; (**c**) blended asphalt binder under the 60 s mixing duration; (**d**) blended asphalt binder under the 90 s mixing duration; (**e**) blended asphalt binder under the 90 s mixing duration; (**f**) aged asphalt binder; (**g**) Variation of density and average area of bee-like structures of blended asphalt with the different mixing duration.

To quantitatively evaluate the influence of mixing duration on blended asphalt binder in the mixing process, the density and the average area of the bee-like structure under different mixing duration were calculated respectively. In Figure 15g, the density of the bee-like structure of virgin asphalt is the largest and the average area is the smallest, while the aging asphalt is the opposite. In addition, it is evident from Figure 15g that the density of the bee-like structures in the blended asphalt decreased with the increase in the mixing duration, while the average area of the bee-like structures showed the opposite trend. Therefore, the mixing duration had a significant effect on the blending of the virgin and aged asphalt during the mixing process.

3.3. Performance of RHMA with Different Mixing Durations
3.3.1. High-Temperature Resistance Test

Figure 16 shows the Marshall stability and flow for RHMA with different mixing durations. According to Figure 16a, the Marshall stability and flow of the RHMA were both affected by the mixing duration, the Marshall stability increasing with the increase in the mixing duration, while the growth trend for the flow decreased with the increase in the mixing duration. Figure 16b shows the rutting test results for RHMA with different mixing durations. As the mixing duration increased, RHMA's dynamic stability increased, and its growth trend decreased with increasing mixing durations, which was consistent with the Marshall stability test results. All the RHMA samples also met the requirements of the JTG F40-2017 specification [27] in terms of the Marshall stability and flow.
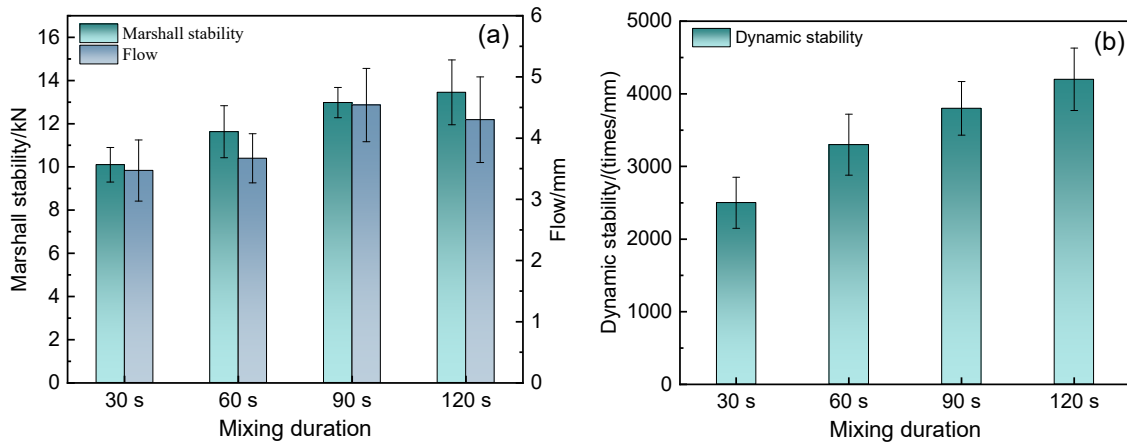
Figure 16. High-temperature resistance test: (**a**) Marshall stability and flow results; (**b**) rutting test results.

3.3.2. Moisture Sensitivity Test

As shown in Figure 17, the splitting tensile strength and splitting tensile strength ratio for the RHMA varied before and after freeze–thawing. Figure 17 shows that the splitting tensile strength before and after the freeze–thaw cycle was affected by the mixing duration. With the increase in the mixing duration, the splitting tensile strength of both the conditioned and unconditioned groups of RHMA samples also increased. In addition, the splitting tensile strength ratio (TSR) for the RHMA increased with the increase in the mixing duration, and the growth trend for the TSR decreased with the increase in the mixing duration. The TSR should be greater than 70% for RHMA containing virgin asphalt according to the JTG F40-2017 specification [27]; therefore, the longer mixing duration was beneficial for RHMA to guarantee moisture stability.
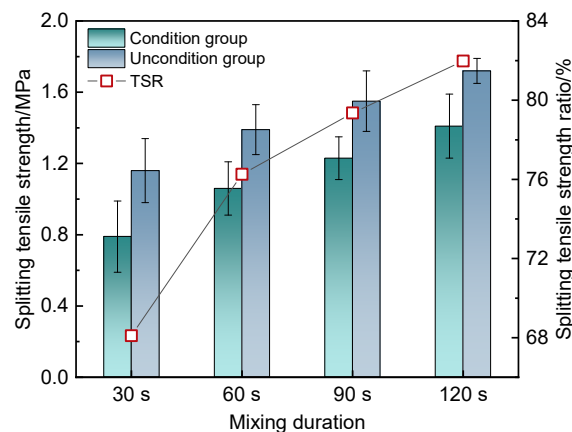

Figure 17. Freeze–thaw splitting results.

3.3.3. Low-Temperature Bending Beam Test

Figure 18 shows that, with an increase in the mixing duration from 30 s to 120 s, the maximum flexural strain of the RHMA increased accordingly. Therefore, the low-temperature crack resistance of the RHMA can be improved by increasing the mixing duration. In addition, the specifications of the JTG F40-2017 standard [27] require a maximum flexural strain not less than 2000 $\mu\varepsilon$. As shown in Figure 18, the RHMA mixed over 30 s, 60 s, and 90 s did not meet the low-temperature performance requirements. Therefore, it is necessary to consider the low-temperature performance of RHMA during the design of the material composition and the mixing process.
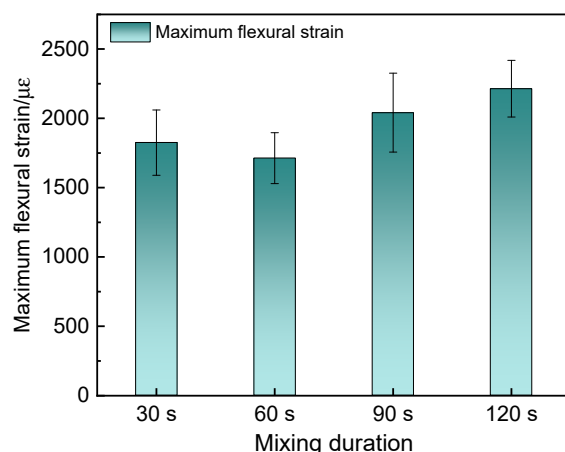
Figure 18. Low-temperature cracking test results.

4. Environmental Impacts

According to findings concerning the energy consumption and carbon emission in the virgin material production stage, transportation stage, mixing stage, and construction stage, the mixing duration can significantly affect the energy consumption and carbon emission of RHMA during the mixing stage. Therefore, the study only compared the difference in energy consumption and carbon emissions during the mixing stage of RHMA. In the context of engineering practice, the Mariani MAT440 and Tietuo TSEC4020 intermittent mixing plants are used to produce RHMA, and the forms of energy consumed in the production process are natural gas and electricity. Statistics show that the natural gas and electricity consumption in the mixing plant can be calculated using Equations (9) and (10), considering an 80% filling rate for the mixer [41]:

$$V_g = -468.731 + 13.193t_m + 2.386T_a + 1.622m_r \tag{9}$$

$$C_e = \frac{P_E \times t_m}{60} \tag{10}$$

where V_g represents the amount of natural gas used in the production of RHMA (m^3); t_m represents the total mixing duration for the production of RHMA (min); T_a represents the discharge temperature of RHMA (°C); m_r represents the total mass for the production of RHMA (ton); P_E represents the total operating power (kW).

Drawing on previous studies [42,43], Table 5 shows the energy consumption and carbon emission equivalents for different types of energy. According to the investigation, the duration of the production cycle for HMA in the plant is 45 s, of which the dry mixing duration is not less than 5~10 s. Therefore, the standard mixing duration for the asphalt mixture can be considered to be 45 s. In addition, the total installed power in the Tietuo TSEC4020 plant is 960 kW. To compare the energy consumption and carbon emissions for RHMA with different mixing durations, their values were calculated for mixing durations of 30 s, 45 s, 60 s, 75 s, and 90 s using Equations (9) and (10), and the results are shown in Table 6. It can be seen that the energy consumption and CO$_2$ emissions for RHMA increase significantly with increasing mixing durations. Comparing the mixing durations of 60 s, 75 s, and 90 s with the standard mixing duration (45 s), the energy consumption for RHMA during the mixing stage increased by 21.5%, 43.3%, and 65.1%, respectively, and the carbon emissions increased by 24.0%, 48.1%, and 72.4%, respectively. Therefore, the optimal mixing duration should be determined considering the energy consumption and carbon emissions at the mixing stage in the plant, as well as the performance of the RHMA.

Table 5. Energy consumption and the CO_2 emissions for different types of energy.

Energy Type	Energy Consumption	CO_2 Emissions
Natural gas	38.931 MJ/m³	2.162 kg/m³
Electricity	3.597 MJ/(kW·h)	0.997 kg/(kW·h)

Table 6. Energy consumption and CO_2 emissions for RHMA produced in a plant with different mixing durations.

Mixing Duration, s	Productivity, t/h	Natural Gas Consumption, m³/t	Electricity Consumption, (kW·h)/t	Energy Consumption, MJ/t	CO_2 Emissions, kg/t
30	480	3.14	2	129.44	8.78
45	320	3.96	3	164.96	11.55
60	240	4.78	4	200.48	14.32
75	192	5.61	5	236.39	17.11
90	160	6.44	6	272.30	19.91

5. Evaluating the Performance of RHMA with Different Mixing Durations in the Plant

To evaluate the performance of RHMA produced in the plant with different mixing durations, an asphalt pavement maintenance project along the Sanming section of the Fuzhou–Yinchuan Expressway in Fujian Province, China, was selected. Considering the operability of different mixing durations in the production of RHMA, the 45 s, 60 s, and 75 s mixing durations were selected for the study, including a dry mixing time of 10 s. The hot mixing duration studied in this work is based on the process used in the intermittent plant mentioned. In RHMA production, the mixing procedure is: (i) RAP premixing for 10 s, (ii) RAP + new aggregates + virgin asphalt mixing for 20 s; and (iii) addition of filler mixture for another 15 s, 30 s, or 45 s. In addition, the material composition of the RAP, the RAP content (40%), and the asphalt content (4.4%) in the RHMA, as well as the aggregate gradation, were consistent with the process in the abovementioned plant. Moreover, the discharge temperature of the RHMA produced in the plant is 170 °C and the compaction temperature for the different test specimens was 155 °C. The performance of the RHMA obtained with different mixing durations was tested, as shown in Figure 19.
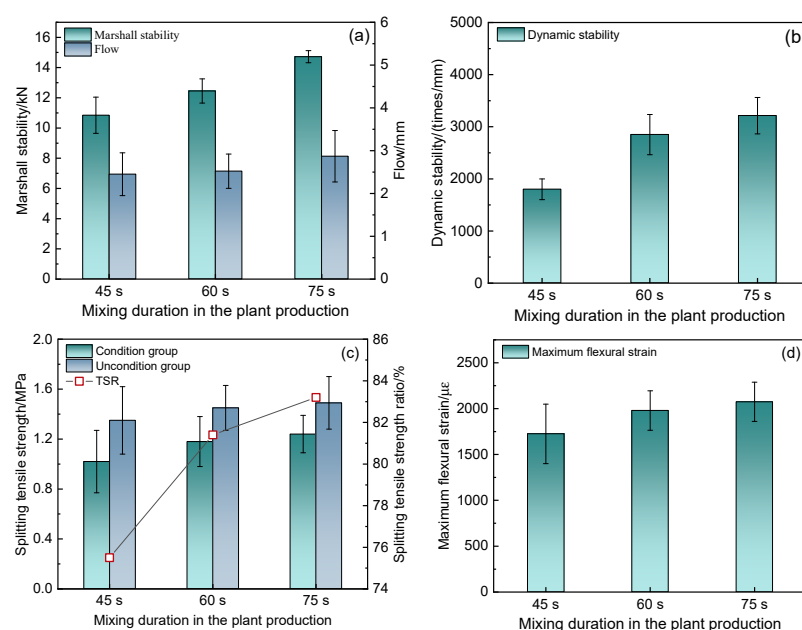
Figure 19. Performance test results for RHMA: (**a**) Marshall stability and flow test; (**b**) rutting test; (**c**) freeze–thaw splitting test; (**d**) low-temperature cracking test.

Regarding the results from Figure 19, the Marshall stability and flow, dynamic stability, freeze–thaw splitting strength ratio, and maximum flexural strain of the RHMA increased with the increase in the mixing duration. However, the growth rate of the different performance indexes decreased with the increase in the mixing duration. In addition, when the mixing duration was 60 s, the performance of the RHMA met the JTG F40-2017 specification requirements. However, the performance of the RHMA did not meet the requirements with the standard mixing duration (45 s). Therefore, to ensure the acceptable performance of RHMA, it is necessary to extend the mixing duration of RHMA compared to virgin asphalt mixture.

6. Discussion of the Results

In this study, the dispersion of reclaimed asphalt and the blending of reclaimed asphalt and virgin asphalt were observed, and the performance of RHMA mixed with different mixing durations was evaluated. In addition, the environmental impact of RHMA produced in a plant with different mixing durations was analyzed, and the performance of RHMA produced in a plant was also evaluated. Furthermore, the optimal mixing duration, taking into account both laboratory tests and the plant, was proposed by considering the environmental impact and the performance of RHMA.

Based on the initial experimental results, the aged asphalt coated on the surface of RAP disperses during the mixing process, and the degree of dispersion increases with the increase in the mixing duration. It was revealed that the mixing process increases the probability of contact between RAP and different virgin aggregates, and the softened, aged asphalt binder coated on the surface of RAP is transferred to the virgin aggregate under the action of adhesion during the mixing process. Therefore, the area of aged asphalt adhering to the surface of virgin aggregate increases with the increase in mixing duration, indicating a more uniform dispersion of RAP during the mixing process. However, this study only qualitatively analyzed the dispersion of RAP in the mixing process without considering the addition of virgin asphalt. According to a previous study [44], when RHMA is added to virgin asphalt, the virgin asphalt tends to attract the smaller RAP particles and coats them first, causing an agglomeration phenomenon for RAP particles during mixing and affecting the RAP dispersion. Hence, the performance and chemical composition of blended asphalt were used to further evaluate the dispersion of RAP.

This study investigated the variation in performance and chemical composition of blended asphalt with different mixing durations. It is known from the literature [31,45,46] that the performance of aged asphalt, in terms of penetration, ductility, phase angle, and creep rate m, are lower compared to virgin asphalt, while the softening point, complex modulus, and stiffness modulus are higher, and both of these trends are due to the change in chemical composition during the aging process. In addition, a previous study [32,33] also revealed that the C=O bond (carbonyl region), S=O bond (sulfoxide), molecular weight distribution, and number of bee-like structures in aged asphalt are affected by the SARA components. As asphalt contains more unsaturated bonds than saturated molecules, small molecules (saturated and aromatic components) break more easily during aging. After the structures of small molecules are broken, they polymerize to form macromolecules (asphaltenes), the molecular weight and modulus of which are greater than those of saturated and aromatic components [47]. Due to the increase in macromolecules, the adhesion and modulus of the asphalt increase. Therefore, the C=O bond, S=O bond, LMS, and area of the bee-like structures have higher peaks as the degree of aging of the asphalt increases. Hence, as the aged asphalt becomes increasingly dispersed into the RHMA during the mixing process, the properties and chemical components of the blended asphalt move closer to those of virgin asphalt. In the practical context, it was observed that the aged asphalt on the RAP surface showed significant dispersion during the mixing process, and the degree of dispersion increased with increasing mixing durations.

Furthermore, it is worth noting that the mixing duration affects the RHMA performance and that the high-temperature stability, moisture sensitivity, and low-temperature

crack resistance of RHMA increase with increases in the mixing duration. In addition, it was observed that the best performance for the RHMA was obtained at a mixing duration of 120 s. Wu et al. [48] reported that a longer mixing duration results in significant age-hardening in both RAP and virgin asphalt binders, as well as a stronger blend of RAP and new binders, meaning that more RAP binder contributes to the viscoelastic properties of RHMA. Therefore, the high-temperature rutting resistance and the moisture sensitivity of RHMA increase. In addition, a longer mixing duration promotes homogeneity in the blending of the aged and the virgin asphalt, and the stress concentration at the interface between the aged and virgin asphalt affecting the crack resistance is reduced, resulting in the low-temperature crack resistance of RHMA increasing with the increase in the mixing duration.

To achieve a higher degree of dispersion of aged asphalt and to guarantee the performance of RHMA, prolonged mixing durations are required during the mixing process. However, in practice, extending the mixing duration of RHMA significantly increases the energy consumption and CO_2 emissions during the RHMA production stage (as shown in Table 6), as well as increasing production costs. Therefore, it is impossible to achieve a sufficient mixing duration, such as 120 s, in the practical production process of RHMA. Although increasing the mixing duration improves the performance of RHMA, it is necessary to consider the actual situation to determine the optimal mixing duration for such projects. In addition, the correlation between the RHMA performances with laboratory and plant mixing durations should be considered to avoid over-evaluation of the performance of the RHMA produced in plants due to the long mixing time used in the laboratory. Thus, it is recommended to balance the performance of RHMA and the environmental benefits of the mixing process to determine an optimal mixing duration. According to the test results for the RHMA produced in the plant (as shown in Figure 19), the optimal mixing duration in the plant is 60 s, considering the environmental impact and the RHMA production efficiency and performance. Furthermore, the optimal mixing duration in the laboratory was determined to be 90 s based on the consistency of the performance of the RHMA mixing in the plant with that of RHMA mixing in the laboratory with different mixing durations. In addition, Haghshenas et al. [46] reported that the mixing temperature affects the dispersion of RAP during the mixing process, and the degree of dispersion increases with the increase in mixing temperature. Karlsson and Isacsson [49] showed that a rejuvenator can promote the dispersion of aged asphalt in RAP during the mixing process. Hence, the abovementioned factors can be considered to improve the degree of RAP dispersion and the performance of recycled asphalt mixes with a limited mixing duration. In addition, the distribution of RAP particles in RHMA during the mixing process is also an interesting topic and its influence on the properties of RHMA should be considered.

7. Conclusions

This study investigated the dispersion and mixing of reclaimed asphalt, evaluated RHMA produced in plants and laboratories, and analyzed the energy consumption and carbon emissions for RHMA with different mixing durations. The dispersion of aged asphalt on the RAP surface with different mixing durations was observed. The performance and chemical composition of blended asphalt recovered from RHMA with different mixing durations were evaluated using physical properties tests, a rheometer test, an FTIR test, a GPC test, and an AFM test. In addition, the performance of RHMA was also evaluated using the Marshall stability test, a rutting resistance test, a freeze–thaw splitting test, and a low-temperature bending beam test. Based on the results, an optimal mixing duration can be proposed. The following conclusions can be drawn for this study:

(1) The dispersion of aged asphalt over the RAP surface in RHMA was significantly influenced by the mixing duration, and the degree of dispersion increased with the increase in the mixing duration. In addition, the mixing duration of RHMA affected the degree of blending of aged and virgin asphalt; the lower the mixing duration was, the lower the degree of blending was. When the mixing duration was increased, the properties

and the chemical composition of the blended asphalt approached those of aged asphalt, indicating that the dispersion of aged asphalt on the RAP surface was greater in the longer mixing process. Furthermore, the high-temperature resistance, moisture sensitivity, and low-temperature crack resistance of RHMA were improved by increasing the mixing duration. In general, the mixing duration affects the dispersion of RAP in RHMA and the blending of the old and new asphalt during the mixing process, thus affecting the performance of the recycled asphalt mixture.

(2) The energy consumption and CO_2 emissions at the production stage of RHMA increased significantly with the increase in the mixing times. In addition, the performance of the RHMA produced in the plant increased with the increase in mixing time. The recommended optimal mixing durations in the mixing plant and laboratory are 60 s and 90 s, respectively, considering the environmental impact and the RHMA production efficiency and performance.

(3) In this study, we considered a single concentration of RAP and the degree of aging of RAP in RHMA, but the results may differ when considering different RAP concentrations or degrees of aging. In order to determine the impact of RAP content and the degree of aging on RHMA performance, it is recommended that these tests be repeated.

References

1. Sha, A.; Liu, Z.; Jiang, W.; Qi, L.; Hu, L.; Jiao, W.; Barbieri, D.M. Advances and development trends in eco-friendly pavements. *J. Road Eng.* **2021**, *1*, 1–42. [CrossRef]
2. Wang, H.; Rath, P.; Buttlar, W.G. Recycled asphalt shingle modified asphalt mixture design and performance evaluation. *J. Traffic Transp. Eng.* **2020**, *7*, 205–214. [CrossRef]
3. Pasetto, M.; Baliello, A.; Giacomello, G.; Pasquini, E. Towards very high RAP content asphalt mixes: A comprehensive performance-based study of rejuvenated binders. *J. Traffic Transp. Eng.* **2021**, *8*, 1022–1035. [CrossRef]
4. Gao, J.; Yang, J.; Yu, D.; Jiang, Y.; Ruan, K.; Tao, W.; Sun, C.; Luo, L. Reducing the variability of multi-source reclaimed asphalt pavement materials: A practice in China. *Constr. Build. Mater.* **2021**, *278*, 122389. [CrossRef]
5. Yang, J.; Tao, W.; Gao, J.; Yu, D.; Zhou, J.; He, L.; Yao, Y. Measurement of particle agglomeration and aggregate breakdown of reclaimed asphalt pavement. *Constr. Build. Mater.* **2021**, *296*, 123681. [CrossRef]
6. Cai, J.; Song, C.; Gong, X.; Zhang, J.; Pei, J.; Chen, Z. Gradation of limestone-aggregate-based porous asphalt concrete under dynamic crushing test: Composition, fragmentation and stability. *Constr. Build. Mater.* **2022**, *323*, 126532. [CrossRef]
7. Wang, D.; Riccardi, C.; Jafari, B.; Falchetto, A.C.; Wistuba, M.P. Investigation on the effect of high amount of Re-recycled RAP with Warm mix asphalt (WMA) technology. *Constr. Build. Mater.* **2021**, *312*, 125395. [CrossRef]
8. Zaumanis, M.; Mallick, R.B.; Frank, R. 100% recycled hot mix asphalt: A review and analysis. *Resour. Conserv. Recycl.* **2014**, *92*, 230–245. [CrossRef]
9. Antunes, V.; Freire, A.C.; Neves, J. A review on the effect of RAP recycling on bituminous mixtures properties and the viability of multi-recycling. *Constr. Build. Mater.* **2019**, *211*, 453–469. [CrossRef]
10. Hou, X.; Hettiarachchi, C.; Xiao, F.; Zhao, Z.; Xiang, Q.; Yong, D. Blending efficiency improvement and energy investigation of recycled asphalt mixture involved warm mix technology. *J. Clean. Prod.* **2021**, *279*, 123732. [CrossRef]

11. Falchetto, A.C.; Moon, K.H.; Kim, D.H. Evaluation of recycled asphalt mixture at low temperature using different analytical solutions. *Can. J. Civ. Eng.* **2020**, *47*, 801–811. [CrossRef]

12. Oualit, M.; Irekti, A.; Hami, B. Performance of recycled asphalt mixtures formulated with modified bitumen. *Environ. Eng. Manag. J.* **2019**, *18*, 2613–2621. [CrossRef]

13. McDaniel, R.; Anderson, R.M. *Recommended Use of Reclaimed Asphalt Pavement in the Superpave Mix Design Method: Technician's Manual*; Transportation Research Board: Washington, DC, USA, 2001; pp. 1–60.

14. Xu, Y.; Chou, Z.; Li, Y.; Ji, J.; Xu, S. Effect of Blending Degree between Virgin and Aged Binder on Pavement Performance of Recycled Asphalt Mixture with High RAP Content. *Adv. Mater. Sci. Eng.* **2019**, *2019*, 5741642. [CrossRef]

15. Ashtiani, M.Z.; Mogawer, W.S.; Austerman, A.J. A Mechanical Approach to Quantify Blending of Aged Binder from Recycled Materials in New Hot Mix Asphalt Mixtures. *Transp. Res. Rec. J. Transp. Res. Board* **2018**, *2672*, 107–118. [CrossRef]

16. Kaseer, F.; Arámbula-Mercado, E.; Martin, A.E. A Method to Quantify Reclaimed Asphalt Pavement Binder Availability (Effective RAP Binder) in Recycled Asphalt Mixes. *Transp. Res. Rec. J. Transp. Res. Board* **2019**, *2673*, 205–216. [CrossRef]

17. Shirodkar, P.; Mehta, Y.; Nolan, A.; Sonpal, K.; Norton, A.; Tomlinson, C.; Dubois, E.; Sullivan, P.; Sauber, R. A study to determine the degree of partial blending of reclaimed asphalt pavement (RAP) binder for high RAP hot mix asphalt. *Constr. Build. Mater.* **2011**, *25*, 150–155. [CrossRef]

18. Vassaux, S.; Gaudefroy, V.; Boulangé, L.; Pévère, A.; Michelet, A.; Barragan-Montero, V.; Mouillet, V. Assessment of the binder blending in bituminous mixtures based on the development of an innovative sustainable infrared imaging methodology. *J. Clean. Prod.* **2019**, *215*, 821–828. [CrossRef]

19. Ding, Y.; Huang, B.; Shu, X. Blending efficiency evaluation of plant asphalt mixtures using fluorescence microscopy. *Constr. Build. Mater.* **2018**, *161*, 461–467. [CrossRef]

20. Bowers, B.F.; Moore, J.; Huang, B.; Shu, X. Blending efficiency of Reclaimed Asphalt Pavement: An approach utilizing rheological properties and molecular weight distributions. *Fuel* **2014**, *135*, 63–68. [CrossRef]

21. Solaimanian, M.; Chen, X. Investigating Degree of Blending Between Reclaimed Asphalt Pavement and Virgin Binder Using Atomic Force Microscopy and Focused Ion Beam. *Transp. Res. Rec. J. Transp. Res. Board* **2021**, *2021*, 036119812110184. [CrossRef]

22. Rinaldini, E.; Schuetz, P.; Partl, M.N.; Tebaldi, G.; Poulikakos, L.D. Investigating the blending of reclaimed asphalt with virgin materials using rheology, electron microscopy and computer tomography. *Compos. Part B Eng.* **2014**, *67*, 579–587. [CrossRef]

23. Xu, J.; Hao, P.; Zhang, D.; Yuan, G. Investigation of reclaimed asphalt pavement blending efficiency based on micro-mechanical properties of layered asphalt binders. *Constr. Build. Mater.* **2018**, *163*, 390–401. [CrossRef]

24. Research Institute of Highway Ministry of Transport. *Standard Test Methods of Bitumen and Bituminous Mixtures for Highway Engineering*; China Communications Press: Beijing, China, 2011; pp. 1–358.

25. Research Institute of Highway Ministry of Transport. *Testing Methods of Aggregate for Highway Engineering*; China Communications Press: Beijing, China, 2005; pp. 1–131.

26. Research Institute of Highway Ministry of Transport. *Technical Specifications for Highway Asphalt Pavement Recycling*; China Communications Press: Beijing, China, 2019; pp. 1–92.

27. Research Institute of Highway Ministry of Transport. *Technical Specifications for Construction of Highway Asphalt Pavements*; China Communications Press: Beijing, China, 2017; pp. 1–186.

28. Yan, C.; Huang, W.; Lin, P.; Zhang, Y.; Lv, Q. Chemical and rheological evaluation of aging properties of high content SBS polymer modified asphalt. *Fuel* **2019**, *252*, 417–426. [CrossRef]

29. Yan, C.; Huang, W.; Tang, N. Evaluation of the temperature effect on Rolling Thin Film Oven aging for polymer modified asphalt. *Constr. Build. Mater.* **2017**, *137*, 485–493. [CrossRef]

30. Baqersad, M.; Ali, H. Rheological and chemical characteristics of asphalt binders recycled using different recycling agents. *Constr. Build. Mater.* **2019**, *228*, 116738. [CrossRef]

31. Hettiarachchi, C.; Hou, X.; Xiang, Q.; Yong, D.; Xiao, F. A blending efficiency model for virgin and aged binders in recycled asphalt mixtures based on blending temperature and duration. *Resour. Conserv. Recycl.* **2020**, *161*, 104957. [CrossRef]

32. Hou, X.; Xiao, F.; Wang, J.; Amirkhanian, S. Identification of asphalt aging characterization by spectrophotometry technique. *Fuel* **2018**, *226*, 230–239. [CrossRef]

33. Hou, X.; Lv, S.; Chen, Z.; Xiao, F. Applications of Fourier transform infrared spectroscopy technologies on asphalt materials. *Measurement* **2018**, *121*, 304–316. [CrossRef]

34. Mirwald, J.; Nura, D.; Hofko, B. Recommendations for handling bitumen prior to FTIR spectroscopy. *Mater. Struct.* **2022**, *55*, 22. [CrossRef]

35. Rathore, M.; Haritonovs, V.; Meri, R.M.; Zaumanis, M. Rheological and chemical evaluation of aging in 100% reclaimed asphalt mixtures containing rejuvenators. *Constr. Build. Mater.* **2022**, *318*, 126026. [CrossRef]

36. Ding, L.; Wang, X.; Zhang, M.; Chen, Z.; Meng, J.; Shao, X. Morphology and properties changes of virgin and aged asphalt after fusion. *Constr. Build. Mater.* **2021**, *291*, 123284. [CrossRef]

37. Nahar, S.N.; Mohajeri, M.; Schmets AJ, M.; Scarpas, A.; Van de Ven, M.F.; Schitter, G. First Observation of Blending-Zone Morphology at Interface of Reclaimed Asphalt Binder and Virgin Bitumen. *Transp. Res. Rec. J. Transp. Res. Board* **2013**, *2370*, 1–9. [CrossRef]

38. Yang, J.; Luo, L.; Gao, J.; Xu, J.; He, C. Study on the Effect of Regeneration Agent on the Viscosity Properties of Aged Asphalt. *Materials* **2022**, *15*, 380. [CrossRef] [PubMed]

39. Rebelo, L.M.; De Sousa, J.S.; Baroni, M.P.M.A.; Alencar, A.E.V.; Soares, S.A.; Filho, J.M.; Soares, J.B. Aging of asphaltic binders investigated with atomic force microscopy. *Fuel* **2014**, *117*, 15–25. [CrossRef]
40. Liu, B.; Shen, J.; Song, X. Changes in Nanoscaled Mechanical and Rheological Properties of Asphalt Binders Caused by Aging. *J. Nanomater.* **2015**, *2015*, 961924. [CrossRef]
41. Meng, X. Study on Quantification of Energy Consumption and Carbon Emission During the Period of Asphalt Pavement Construction. Master's Thesis, Beijing Jiaotong University, Beijing, China, 2020.
42. *GB/T 2589-2020*; General Rules for Calculation of the Comprehensive Energy Consumption. China Communications Press: Beijing, China, 2021; pp. 1–12.
43. China Emission Accounts and Datasets, CEADs. Available online: https://www.ceads.net.cn/data/ (accessed on 10 June 2022).
44. Bowers, B.F.; Huang, B.; Shu, X.; Miller, B.C. Investigation of Reclaimed Asphalt Pavement blending efficiency through GPC and FTIR. *Constr. Build. Mater.* **2014**, *50*, 517–523. [CrossRef]
45. Xing, C.; Liu, L.; Li, M. Chemical Composition and Aging Characteristics of Linear SBS Modified Asphalt Binders. *Energy Fuels* **2020**, *34*, 4194–4200. [CrossRef]
46. Haghshenas, H.F.; Rea, R.; Reinke, G.; Zaumanis, M.; Fini, E. Relationship between colloidal index and chemo-rheological properties of asphalt binders modified by various recycling agents. *Constr. Build. Mater.* **2022**, *318*, 126161. [CrossRef]
47. Wang, J.; Wang, T.; Hou, X.; Xiao, F. Modelling of rheological and chemical properties of asphalt binder considering SARA fraction. *Fuel* **2019**, *238*, 320–330. [CrossRef]
48. Wu, J.; Liu, Q.; Wang, Y.; Chen, J.; Wang, D.; Xie, L.; Ago, C. Effect of Mixing duration and Temperature on the Homogeneity of Asphalt Mixtures Containing Reclaimed Asphalt Pavement Material. *Transp. Res. Rec. J. Transp. Res. Board* **2018**, *2672*, 167–177. [CrossRef]
49. Karlsson, R.; Isacsson, U. Application of FTIR-ATR to Characterization of Bitumen Rejuvenator Diffusion. *J. Mater. Civ. Eng.* **2003**, *15*, 157–165. [CrossRef]